

Design, Modeling, and Optimization of Precision Bent Refocus Optics - LCLS AMO KB Mirror Assembly

Nicholas Kelez¹, John Bozek³, Yi-De Chuang², Robert Duarte¹, D.E. Lee¹, Wayne McKinney², Valeriy Yashchuk², Sheng Yuan²

¹ Engineering Division, Lawrence Berkeley National Laboratory, Berkeley, CA; ² Advanced Light Source, Lawrence Berkeley National Laboratory, Berkeley, CA;

³ Linac Coherent Light Source, Stanford Linear Accelerator Center, Menlo Park, CA;



Abstract

There is an increasing demand for highly de-magnified and well-focused beams with high quality imaging of the full field to further explore the potential of novel instruments. For beamlines operating at a focal point, mechanical benders have often been used to shape the refocusing mirror into an ideal elliptical form. However, the limited number of couplings for these mechanisms requires specific substrate side-shaping, often calculated using beam bending theory, to meet demanding figure requirements. Here, we seek to develop a methodology for rational design and performance evaluation of x-ray optics and their associated bender mechanisms. To this end, finite element analysis (FEA) is used to both validate the side-shaping algorithm and then couple the output with SHADOW® [1] and a bender couple optimization algorithm to evaluate the resulting mirror figure. Finally, the metrology results of the Long Trace Profiler (LTP) are used to both set the final shape of the completed assembly and validate or improve the model and analysis methods.

Step 1:

The distance from the source to the mirror (u), image distance (v) and grazing angle (θ), are determined based primarily on energy, substrate material, coating, performance requirements and beamline configuration constraints. The desired elliptical shape of the mirror, as given by the major axis a , minor axis b and ellipticity e , can be calculated according to:

$$a = (u + v) / 2$$

$$e = \frac{\sqrt{u^2 + v^2 + 2uv \cos(2\theta)}}{(u + v)^2}$$

$$b^2 = a^2(1 - e^2)$$

Subsequently, one can show that the position on the elliptical mirror section can be approximated by the tangential line through the mirror pole (x_p, y_p) :

$$x(p) = \frac{p}{\sqrt{1 + (x_p^2/b^2 - y_p^2/a^2)}(a^2 - x_p^2)} + x_0$$

From [2], the bending moment is the double integral of the gravitational force per unit length. Therefore, the bending moment at point p becomes:

$$M(p) = \frac{1}{2} \left[C_1 \left(\frac{L}{2} - p \right) + C_2 \left(\frac{L}{2} + p \right) \right] + \rho g \int_{-L/2}^p \int_{-L/2}^x w(x') dx' dx' + Ap + B$$

where $C_{1,2}$ are the moments for up- and downstream ends and A and B are the integration constants to ensure zero gravity contribution at both ends. The width profile, with constant thickness, is then calculated by iterating the following equation with the bending moment equation shown above:

$$w(p) = \frac{12M(p)}{E t^3 (p) \kappa_{eff}}$$

where κ is the curvature and E is the bulk modulus [2]. Consistent width profiles are generally obtained within several iterations.

The calculated width and corresponding couples are then modeled in the FEA program ANSYS® to validate the width profile. In his process, the model is constructed with pure bending moments $C_{1,2}$ applied about the neutral axis of the mirror end surfaces. Constraints are then applied such that the upstream end is fully constrained in translation (x, y, z) and the downstream end is constrained in elevation (y) only. The resulting deformed surface is compared with the ideal elliptical surface and the difference is calculated with polynomial fitting to minimize numerical errors from small changes. This mesh is used as an input for PRESURFACE [3-5] and the output binary file is then used to modify the mirror surface in SHADOW.

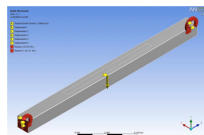


Figure 1: FEA Model of ideal substrate bending.

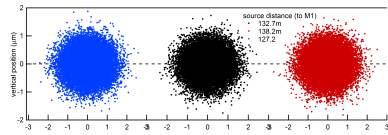


Figure 2: SHADOW ray trace of the focus resulting from deformed shape of the FEA simulation.

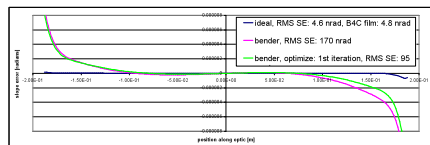


Figure 3: RMS slope plots of 3 different levels of simulation.

The demanding figure requirements (<2 microradian RMS) necessitated a silicon substrate (~.1 microradian RMS polished flat) and the minimum bent radius required a nominal thickness of 25mm to keep the maximum bending stress <2.5ksi. Based on this thickness, we selected glued end blocks as the mechanism for applying the desired bending couples.

System functional requirements included operating at multiple foci, plane transmission (flat), and B4C substrate coating. As a result, the design incorporated external motorized pulling stages, internal strong-back support with LVDT displacement measurement of the deformed cantilever springs, and a unique 45 degree vacuum chamber that permits measurements of the completed system on the Long Trace Profiler (LTP) – see Fig. 4.

Step 2:

In the next step, we seek to design a bender mechanism that preserves the ideal form of the bent substrate achieved in Step 1. As an example, we consider the KB Mirror Assembly for the AMO Branchline at the LCLS with the following parameters shown in Table 1.

M1 (horizontal beam mirror)	
Source distance (m)	127.2 - 136.2 (average is 132.7)
Image distance (m)	136
Incidence angle	18.260°
Profile	Elliptical cylinder (after bending the flat)
Elliptical radius	126.7 (m, meridians)
Sagittal radius	400
Mirror length (mm)	400
Mirror width (mm)	-25
Mirror thickness (mm)	25
Tangential shear aperture (mm)	200
Sagittal shear aperture (mm)	10
Tangential slope error (rad)	-0.7
Sagittal slope error (rad)	-0.7
M2 (vertical beam mirror)	
Source distance (m)	127.2 - 136.7 (average is 133.5)
Image distance (m)	136
Incidence angle	18.260°
Profile	Elliptical cylinder (after bending the flat)
Elliptical radius	126.7 (m, meridians)
Sagittal radius	400
Mirror length (mm)	400
Mirror width (mm)	-25
Mirror thickness (mm)	25
Tangential shear aperture (mm)	200
Sagittal shear aperture (mm)	10
Tangential slope error (rad)	-0.7
Sagittal slope error (rad)	-0.7

Table 1: LCLS KB Mirror summary data.

Additionally, particular attention was devoted to maintaining bending mechanism symmetry, minimization of glued interface stresses and bending effects, and mitigation of any non-ideal bending couple forces (e.g. tangential compression or tension forces).

The resulting design concept was then simulated in ANSYS® and assembly tolerances quantified by modeling ranges of mis-alignment and fabrication errors.

Step 3:

The next step after fabrication and assembly to desired tolerances is setting the required optimum shape and indexing the LVDT(s). This process takes place on the LTP in the Optical Metrology Lab (OML) at the Advanced Light Source (ALS) where the group has developed a novel method for quickly setting the ideal bending couples; this process was also used in the FEA simulations of the complete bender.

The method consists of only three slope traces measured before and after a single adjustment of each bending couple. An algorithm is used in dedicated software for finding optimal settings for the mirror benders. The algorithm is based on a method of regression analysis that experimentally found characteristic functions of the benders (see Fig. 7). The resulting approximation to the functional dependence of the desired slope shape provides nearly final settings for the benders. Moreover, the characteristic functions of the benders found in the course of tuning, can be used for retuning of the optics to a new desired shape without removing from the beamline and re-measuring with the LTP [6].

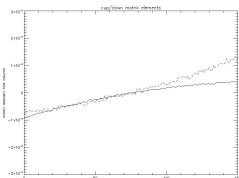


Figure 7: Characteristic functions of LCLS AMO KB M2 mirror assembly.

Results from the initial bending of the mirror assemblies, shown in Figure 8, were quite good (~2 microradian RMS) and primarily limited by the current capabilities of the LTP and schedule constraints.

Further system characterization on the LTP included stability and repeatability measurements. For stability, the system was examined with 3 sets of high resolution (8 pass) scans spanning a 24 hr period that showed drift in the range of 17000km.

Investigation of repeatability involved relaxing the benders to the flat substrate form and then returning the displacement springs to the nominal LVDT values identified during bending optimization. Results showed nearly identical slope deviations (~2 microradians) and only a small defocus form of 197 km leading to a shift in the focal plane on the order of microns.

Step 4:

The LCLS AMO KB Mirror System recently completed metrology and final assembly tasks and is scheduled to begin installation 8/24/09. The final step of this process will be to use the empirical results of the actual system to validate and improve the simplifications and assumptions of the modeling process. In particular, we will focus on correlating both the actual cantilever spring displacements and system sensitivity to changes in couples with those predicted by our simulations.

References

- [1] SHADOW ray-tracing code was developed by center for nanotechnology (CNTech). See http://www.nanotech.wisc.edu/CNT_LABS/shadow.html
- [2] E.P. Popov, Engineering Mechanics of Solids, Prentice Hall, Englewood Cliffs, NJ.
- [3] M. Sanchez del Rio and A. Marcelli, Nucl. Instrum. Meth. Phys. Res. A 319, 170-177 (1992).
- [4] M. Sanchez del Rio, Rev. Sci. Instrum. 67, 1-6 (1996).
- [5] Instead of using the waveness command as suggested in reference [3] and [4], we use the PRESURFACE directly.
- [6] W. McKinney et al., Optimal tuning and calibration of bendable mirrors with slope measuring profilers, Optical Eng. (2008)

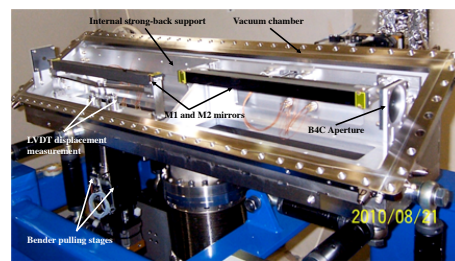


Figure 4: Completed KB assembly with vacuum chamber lid removed.

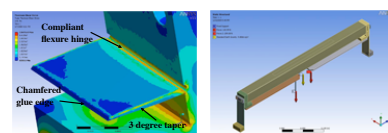


Figure 5: End block optimization simulation.

Figure 5: Assembly and fabrication modeling.

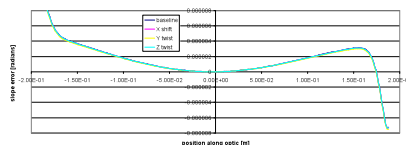


Figure 6: Results of assembly and fabrication tolerance simulations

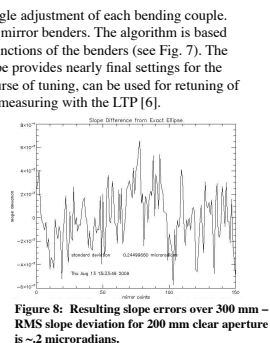


Figure 8: Resulting slope errors over 300 nm - RMS slope deviation for 200 nm clear aperture is ~2 microradians.